Available online at www.sciencedirect.com
SCIENCE DIRECT®
Steroids 69 (2004) 235–243
Steroids
www.elsevier.com/locate/steroids

Characterization of stable human aromatase expressed in *E. coli*

Norio Kagawa [a,*], Hiroshi Hori [b], Michael R. Waterman [a], Shiro Yoshioka [a,1]

[a] *Department of Biochemistry, Vanderbilt University School of Medicine, Nashville, TN 37232-0146, USA*
[b] *Division of Bioengineering, Graduate School of Engineering Science, Osaka University, Toyonaka, Osaka 560-8531, Japan*

Received 13 November 2003; received in revised form 15 January 2004; accepted 20 January 2004

Available online 12 May 2004

Abstract

Aromatase (P450arom, CYP19) catalyzes the aromatization reaction that converts androgens to estrogens. Although human P450arom has been readily purified from placenta, its hydrophobic properties and instability has hampered detailed characterization. Utilizing a N-terminal replacement (MARQSFGRGKL, derived from CYP2C11), we successfully modified this unstable enzyme into stable forms. Based on a known polymorphism, we created two constructs, NmA264C and NmA264R having cysteine or arginine at position 264. The recombinant P450arom NmA264R was expressed in *Escherichia coli* (350–400 nmol/L culture) primarily by coexpression with molecular chaperones GroES/GroEL while NmA264C was expressed (240 nmol/L culture) only in the presence of chloramphenicol. Although NmA264C was recovered only in the membrane fraction, approximately 14% of NmA264R was recovered in the cytosolic fraction, suggesting that NmA264R is more hydrophilic than NmA264C. NmA264R was highly purified to the specific content 13.6 nmol P450/mg protein. Purified P450arom NmA264R converted androstenedione to estrone with V_{max} 12.4 nmol/(min nmol) and K_m 0.26 μM, and testosterone to estradiol with V_{max} 52.2 nmol/(min nmol) and K_m 10.9 μM. Because of the increased stability of NmA264R, we could unambiguously determine properties of human P450arom by optical and electron paramagnetic resonance spectroscopy. The purified protein was a typical low-spin form, which was converted to a high-spin form when androstenedione was added. The rhombicity of substrate-bound forms was higher than that reported for other P450s, an interesting characteristic of human P450arom. The highly stable and active P450arom NmA264R sets the stope for detailed structure/function analyses of this important member of the P450 superfamily.

Keywords: Estrogen; Androgen; EPR; Polymorphism; Aromatase inhibitors

1. Introduction

Estrogens are produced by aromatization of androgens in peripheral tissues by aromatase (P450arom, the product of the *CYP19* gene), a member of the cytochrome P450 superfamily. This enzyme is widely distributed in gonads and extragonadal tissues, including ovary, testis, brain, skin, and adipose tissue [1,2]. In pre-menopausal women, the ovaries are the principle source of estrogen. However, in post-menopausal women and in men, estrogen is produced in a number of extragonadal sites where it acts locally, including the mesenchymal cells of adipose tissue [3,4], osteoblasts and chondrocytes of bone [5–7], the vascular endothelium and aortic smooth muscle cells [8,9], and numerous sites in the brain [10,11]. P450arom is of great interest because of its involvement in essential physiological events and correlation with estrogen-related disease. In particular, breast cancer is correlated with the local production of estrogen from the aberrant expression of P450arom in adipose stromal cells [12], which has led investigators in the related fields to develop potent and specific aromatase inhibitors as drugs for management of breast cancer in post-menopausal women.

P450arom converts androstenedione and testosterone to estrone and estradiol. The stoichiometry of the reaction was shown to be 3 mol of oxygen and 3 mol of NADPH for each mol of estrogen formed [13]. The first and second oxidative steps occur at the 19-carbon of androgens. The final oxidation provides the trigger for concerted elimination of the oxidized C19 residue as formic acid [14] together with stereospecific elimination of the 1β and 2β hydrogen atoms from the A-ring [15,16]. The mechanism of the complex third step remains obscure. Unlike other reactions catalyzed by P450 enzymes, carbon monoxide (CO) does not inhibit the aromatization reaction of androstenedione [17]. This lack of inhibition by CO is not yet understood.

* Corresponding author. Tel.: +1-615-343-1372; fax: +1-615-322-4349.
E-mail address: norio.kagawa@vanderbilt.edu (N. Kagawa).
[1] Present address: Institute for Molecular Science, Okazaki National Research Institute, Okazaki, Aichi 444-8585, Japan.

0039-128X/$ – see front matter © 2004 Elsevier Inc. All rights reserved.
doi:10.1016/j.steroids.2004.01.002

Detailed characterization of P450arom is of interest not only because of the complex nature of the aromatization reaction, but also because of the importance of developing potent inhibitors for use in the treatment of breast cancer and other estrogen-related diseases [1]. Human P450arom has been purified and characterized from placenta by several groups [18–24]. Because of its instability, this membrane protein has required presence of detergents and substrates throughout purification steps. Furthermore, determination of P450 content during purification was unusual in that the presence of 19-norandrostenedione but not androstenedione allowed carbon monoxide to ligate the heme-iron [25]. The hydrophobic nature and unusual instability has hampered obtaining sufficient quantities of highly purified P450arom for detailed structure-function studies. Heterologous expression of cDNA clones encoding the human P450arom [26,27] utilizing baculovirus [28–32] and *Escherichia coli* [33,34] systems with and without modification has been studied for ease of purification of human P450arom. However, the expression levels were too low to obtain large amounts of human P450arom.

Expression conditions of more than 60 microsomal mammalian P450s in *E. coli* suggest that deletion of the membrane anchor and replacement of the "basic-region" with that of a well-expressed P450 can facilitate the expression of those forms originally found difficult to express in *E. coli* [35]. Further, we have shown that the use of cold stress [36] and osmotic stress response [37] in *E. coli* can facilitate expression of heterologous proteins [38,39]. Utilizing the accumulated knowledge for *E. coli* expression systems, human P450arom has been efficiently expressed in *E. coli* by N-terminal replacement and the induction of cold stress response by chloramphenicol [40]. We have now compared the expression of two forms of human P450arom created based on a known polymorphism leading to an amino acid difference at position 264, cysteine or arginine. This difference was found to alter the pattern of expression in *E. coli*. The N-terminal modified P450arom having arginine at 264 (NmA264R) can be efficiently expressed in *E. coli* and purified as a stable form which can be studies catalytically and by biophysical techniques.

2. Materials and methods

2.1. Construction of P450arom-expression plasmids

The GroES/GroEL expression plasmid pGro12 was obtained from Dr. T. Yura, HSP Research Institute, Kyoto [41]. Polymorphism of CYP19 was searched in the NCBI databank, SNP program. The expression plasmid NmA264CpCW was previously described [40]. The NmA264RpCW was created by site-directed mutagenesis using Quick Change (Stratagene) and NmA264CpCW as a template. The mutagenic primers were a forward primer 5′-ATAGCAGAAAAAAGACGCAGGATTTCCACAGAAGAGAAACTG-3′ and a reverse primer 5′-TCCTGCGATCTTTTTTCTGCTATCAGAACTTCTATGGCATCTTTC-3′. The nucleotide sequences were determined by automated sequencing.

2.2. Expression and extraction of P450arom

We used a small culture (25 ml) for examination of the expression level and a large one (250 ml) for protein preparation. We describe here the 250 ml culture as our standard method. *E. coli* DH5α cells transformed with the expression plasmids were incubated at 37°C overnight in 5 ml TB media supplemented with 100 μg/ml ampicillin. The overnight culture (2 ml) was diluted into 250 ml TB media in 3 L culture flask and incubated for 4 h at 37 °C. After addition of 1 mM IPTG, 1 mM δ-aminolevulinic acid (a heme precursor), and 1 μg/ml chloramphenicol for induction of cold stress response or 4 mg/ml arabinose for induction of molecular chaperones GroES/GroEL, the culture was further incubated at 28 °C for 38 h.

Cells were harvested by centrifugation and treated on ice for 30 min with 0.5 mg/ml lysozyme in a buffer containing 50 mM Tris–HCl (pH 7.2), 250 mM sucrose, and 0.5 mM EDTA [42]. After centrifugation, spheroplasts were sonicated in buffer A (100 mM potassium phosphate (pH 7.4), 500 mM sodium acetate, 0.1 mM EDTA, 0.1 mM DTT, 20 % glycerol, 1.5% sodium cholate, 1.5% Tween 20, 1 μM androstenedione, and 100 μM phenylmethylsulfonyl fluoride (PMSF)). The cell lysates were centrifuged at 95,000 rpm for 10 min (Beckman TL-100 ultracentrifuge, TLA-100.4 rotor) and supernatants were pooled for the purification after determination of total proteins using the BCA protein assay kit (Pierce) and P450 content by the reduced CO-difference spectrum [40]. To isolate the cytosolic and membrane fractions, spheroplasts were sonicated in the buffer A without detergents and centrifuged at 95,000 rpm for 10 min. After separation of supernatants as cytosolic fractions, pellets were again sonicated in the buffer A containing the detergents and centrifuged in the same manner. The supernatants were analyzed as solubilized membrane fractions.

2.3. Purification of expressed P450arom

All column chromatography were carried out using Econo-Column 2.5 cm i.d. (Bio-Rad) with gravity flow. The *E. coli* extracts (approximately 4.6 g total protein from 4 × 250 ml culture that contained 390 nmol P450) were applied on a Ni-NTA agarose column (20 ml packed-bed volume) equilibrated with buffer A and washed with 4 vol of buffer A plus 16 mM imidazole. After washing with 1 vol of buffer B (70 mM potassium phosphate (pH 7.4), 0.1 mM EDTA, 0.1 mM DTT, 20% glycerol, 0.5% sodium cholate, 1% Emulgen 913, 1% Tween 20, 1 μM androstenedione, and 100 μM PMSF), proteins were eluted at 0.5 ml/min of flow rate with buffer C (100 mM imidazole-acetate (pH

7.4), 0.1 mM EDTA, 0.1 mM DTT, 20% glycerol, 0.6% sodium cholate, 1% Emulgen 913, 1% Tween 20, 1 μM androstenedione, and 100 μM PMSF). The dark red fractions were pooled and loaded at 0.5 ml/min of flow rate on a DEAE-Sepharose Fast Flow (Amersham Pharmacia Biotech) column (20 ml packed-bed volume) equilibrated with buffer B without androstenedione, and the column was washed at 0.5 ml/min of flow rate with buffer B without androstenedione. The pass-through fractions were diluted with 1 vol of a solution (0.1 mM EDTA, 0.1 mM DTT, 20% glycerol, 0.6% sodium cholate, and 1% Tween 20) that is adjusted to pH 7.4. The diluted sample was applied on a hydroxyapatite (Bio-Rad) column (15 ml packed-bed volume) equilibrated with the buffer D (30 mM potassium phosphate (pH 7.4), 0.1 mM EDTA, 0.1 mM DTT, 20% glycerol, 0.6% sodium cholate and 1% Tween 20). The column was washed with 4 vol of buffer D to remove P420 and eluted at 0.2 ml/min of flow rate with a linear gradient (100 ml) of 30–200 mM sodium phosphate (pH 7.4) that contained 0.1 mM EDTA, 0.1 mM DTT, 20% glycerol, 0.6% sodium cholate, and 1% Tween 20. P450arom (NmA264R) was eluted at 70–120 mM sodium phosphate, yielding 32–38% recovery of P450 from the starting extracts. The fractions (higher than 50 μM P450) were pooled and frozen in liquid nitrogen for storage at −80 °C. Because imidazole binds heme-iron and interferes with determination of P450 by reduced CO-difference spectrum, P450 content was determined only in the starting extracts and fractions obtained from the hydroxyapatite column. During the purification steps, therefore, red colored fractions were collected without monitoring absorption.

2.4. Reconstitution and measurement of aromatase activity

Aromatase activity was reconstituted with purified rat P450 reductase expressed in *E. coli* [43,44]. The standard assay was performed at 37 °C using 3 pmol P450arom, 7.5 pmol P450-reductase in 650 μl reaction buffer containing 50 mM potassium phosphate (pH 7.4), 50 μM dilauroyl-phosphatidylcholine (DLPC), 1 mM glutathione. The reaction was initiated by addition of NADPH (1 mM final). The radioactive substrates, [4-^{14}C]-androstenedione and [4-^{14}C]-testosterone were purchased from American Radiolabeled Chemicals Inc. At each time point, 100 μl reaction mixture was transferred into 100 μl of 5 M guanidine thiocyanate and extracted twice with 1ml of toluene. The toluene extracts were combined, dried under air, and dissolved in 50 μl ethanol. The reaction products were displayed on a thin layer chromatographic plate (PE SIL G, Whatman) with ethyl acetate/dichloromethane 4:6 for androstenedione and 3.5:6.5 for testosterone. The reaction was analyzed using both phosphorimager (Personal Molecular Imager FX, Bio-Rad) and liquid scintillation counter (Wallac 1409, Pharmacia).

2.5. Electron paramagnetic resonance (EPR) spectroscopy

Measurement of EPR was carried out at X-band (9.22 GHz) microwave frequency by using a Varian E-12 EPR spectrometer equipped with an Oxford Instruments ESR-900 continuous flow cryostat system [45,46]. The detection of ferric heme species was performed under the condition, 10 mW microwave power, 100 kHz field modulation with 0.1 mT amplitude, and temperature at 15 or 5 K. The rhombicity values were calculated as $6.25 \times (g_x - g_y)$ [47].

2.6. Other methods and materials

Results presented are from a representative experiment and each experiment was performed at least three times to yield comparable results. Bacto Tryptone and Bacto Yeast Extract Technical were purchased from Difco. Spectral data, kinetic parameters, and statistics were analyzed using a software Igor Pro 4.0 (Wavemetrix Inc.).

3. Results

3.1. Comparison of two forms of human P450arom

Based on a known polymorphism of human P450arom, amino acid 264 can be cysteine (previously expressed form NmA264C [40]), histidine, or arginine. The hydrophilicity profile of Nm264C shows a peak value of 1.60 in the G–H loop at position R265 (Fig. 1C). The highest hydrophilic peak of this protein is at D290 (peak value 2.3) in the H–I loop. When the C264 is replaced by arginine, the peak value at R265 is 2.38. To examine whether this difference in hydrophilicity profiles might influence expression, the two forms of human P450arom (Fig. 1A and B) were expressed in *E. coli*. Both contained a C-terminal 4xHis-tag. As shown in Fig. 2, NmA264C was expressed in the presence of 1 μg/ml chloramphenicol (240 nmol/l culture), and no detectable P450 was recovered in cytoplasmic fractions. The coexpression of GroES/GroEL was not effective for enhancing the expression of NmA264C. In contrast, the expression of NmA264R was greatly enhanced by the coexpression of GroES/GroEL to reach the level of 400 nmol/l culture although it was not enhanced by chloramphenicol. The NmA264R was recovered in both cytoplasmic (14 ± 6%) and membrane fractions (86 ± 6%), suggesting decreased hydrophobicity compared with NmA264C. Because of the higher expression level and decreased hydrophobicity, we have used NmA264R for further studies.

3.2. Purification of human P450arom NmA264R

Because a portion of NmA264R was recovered in cytoplasmic fractions, this protein might be purified without de-

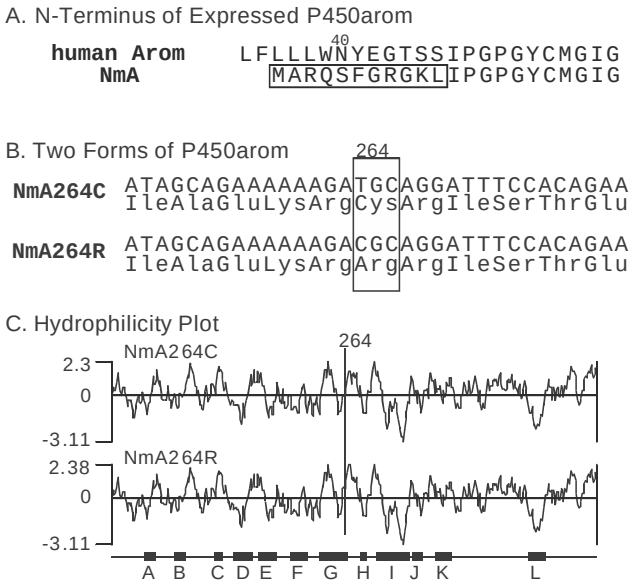

Fig. 1. Sequences of expression constructs. (A) Schematic comparison of human P450arom and the N-terminal sequence of the expression constructs. In the expression constructs, the first 46 N-terminal amino acids of human P450arom (human NmA) were replaced by MARQSFGRGKL (boxed) from rat CYP2C11 [64]. (B) The difference in amino acid and nucleotide sequences between NmA264R and NmA264C. (C) Hydrophilicity plots of NmA264C and Nm264R determined by Protean (DNASTAR) are compared. The schematic structure below the plots shows predicted locations of α-helices [65].

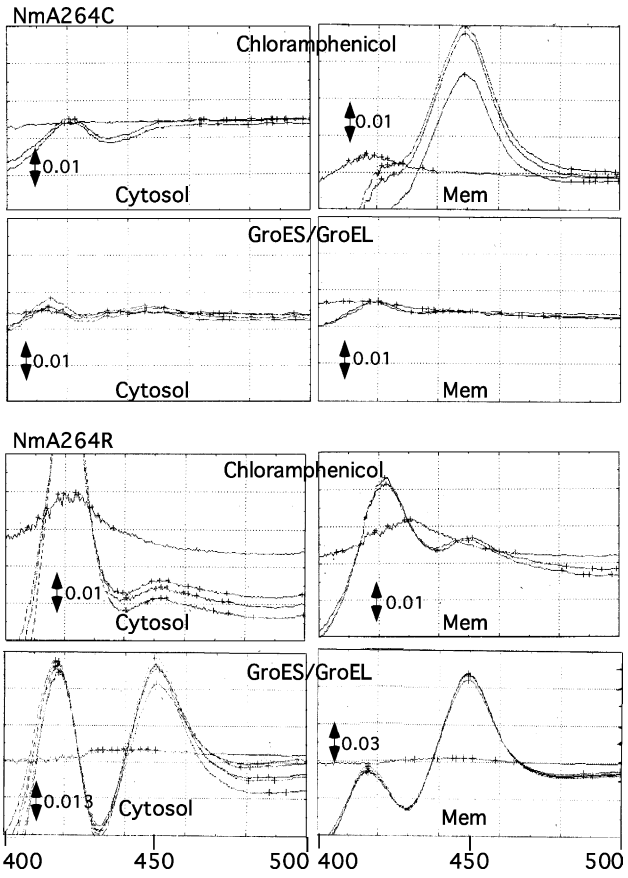

Fig. 2. Expression levels of two forms of human P450arom and distribution between cytoplasmic and membrane fractions. The human P450arom was expressed in 25 ml cultures as described in Section 2. Chloramphenicol (1 μg/ml) or arabinose (4 mg/ml) was added simultaneously with IPTG and δ-aminolevulinic acid. After 38 h incubation at 28 °C, 10 ml of cultures were harvested and the expression levels of P450 determined by reduced CO-difference spectra.

tergent. Therefore, the cytoplasmic fractions of NmA264R were applied on a Ni-NTA column for purification. However, elution of this protein in the P450 form required detergents. Therefore, we solubilized *E. coli* spheroplasts with detergent-containing buffer by sonication for purification of total P450arom using Ni-NTA agarose, DEAE-Sepharose, and hydroxyapatite column chromatography. NmA264R was purified in the absence of substrates to the specific content 13.4 nmol P450/mg protein (the theoretical specific content 18.4 nmol P450/mg protein), suggesting approximately 73% in purity. The purified P450arom showed the major band at molecular weight 51 kDa (54.4 kDa deduced from the primary sequence) with a minor contaminant at higher molecular weight (Fig. 3A). Although the reduced form of this protein was unstable, the reduced CO-complex of P450arom NmA264R was stable in the absence of 19-norandrostenedione or α-naphthoflavone, showing a peak at 449 nm in the reduced CO-difference spectrum without a detectable shoulder at 420 nm (Fig. 3B).

3.3. Activities of the purified P450arom

Because the engineered protein might produce unexpected side-products, the aromatization reaction was displayed on a TLC plate instead of utilizing the ^{3}H-H_2O detection method [48]. Aromatization activities were analyzed using [4-^{14}C]-labeled substrates. As shown in Fig. 4A, androstenedione was converted to estrone without detectable amounts of intermediates or side-products measured by either phosphorimaging or scintillation counting. Testosterone was also predominantly converted to estradiol. Michaelis–Menten analysis of the aromatization reaction suggests that the human P450arom prefers androstenedione to testosterone as a substrate at lower concentration of androgens (Fig. 4B). The kinetic parameters K_m and V_{max} were 0.26 μM and 12.4 nmol/(min nmol) P450 for androstenedione, and 10.9 μM and 52.2 nmol/(min nmol) P450 for testosterone (Table 1). The kinetic parameters obtained from this study and previous studies [18,21] vary from one another, perhaps due to differences in assay conditions.

3.4. Optical spectroscopic properties of human P450arom

In previous reports [18–24], substrates were used throughout purification steps of P450arom for stabilization, which made it difficult to characterize the substrate-free form of P450arom. In this study, P450arom NmA264R purified in the absence of substrates was sufficiently stable for analysis of spectral properties. Substrate-free P450arom exhibits a

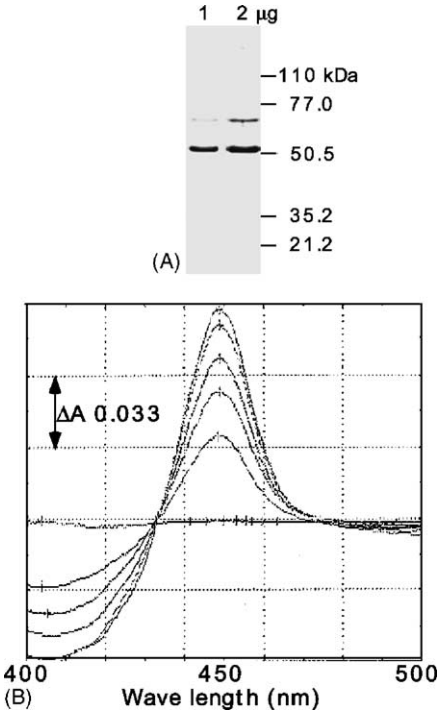

Fig. 3. Properties of purified NmA264R. (A) Purified NmA264R was displayed on a SDS–polyacrylamide gel (10%) and visualized by Coomassie brilliant blue staining. (B) Reduce CO-difference spectrum of an eluted P450arom (NmA264R) from a hydroxyapatite column determined as described in Section 2. Because the reduction of this P450 by sodium dithionite was relatively slow, the sample was scanned several times until the absorbance at 450 reached a maximum.

Soret maximum at 417 nm, α-band at 570 nm, and β-band at 537 nm, indicating that the majority of heme-iron of the purified P450arom is in a typical low-spin state (Fig. 5). The values are consistent with those obtained with the 9-hydroxy-α-naphthoflavone ligated form reported by Kellis and Vickery [21]. The Soret peak was shifted to 395 nm and a charge-transfer band at 645 nm appeared upon addition of androstenedione, indicating a typical high-spin state induced by substrates.

Spectral properties induced by aromatase inhibitors were also investigated. Similar to androstenedione, 4-hydroxyandrostenedione (4-OH-And in Fig. 5), a steroidal aromatase inhibitor, induced a high-spin spectrum. The azole compounds Fadrozole (a second generation aromatase inhibitor) and Femara (or Letrozole) (a third generation aromatase inhibitor) shifted the Soret peak from 417 to 424 nm and 421 nm, respectively. Both inhibitors shifted the β-band to 545 nm and did not show a clear α-band. These shifts of Soret peak and decreased absorbance of α-band by the inhibitors indicated that the nitrogen atom of the azole compounds interacts with the heme-iron as a sixth ligand [49,50].

On substrate-binding difference spectra, androstenedione had higher capacity to induce high-spin spectra than testosterone, as seen in Fig. 7. The addition of androstenedione

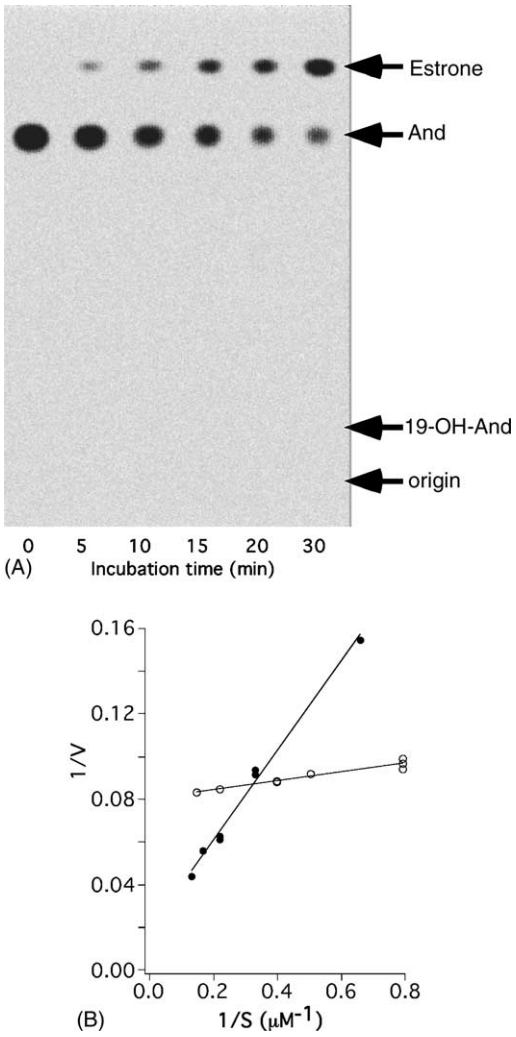

Fig. 4. Aromatization reaction of human P450arom. (A) P450arom (3 pmol) was mixed with NADPH-dependent P450 reductase (7.5 pmol) and ^{14}C-labeled androstenedione (0.82 nmol) in the reaction buffer (0.65 ml) described in Section 2. After addition of NADPH (100 μM), the reaction mixture (0.1 ml) was transferred into a new tube, extracted, and sterols were displayed on a TLC plate, visualized by a phosphorimager. And, androstenedione; 19-OH-And, 19-hydroxyandrostenedione. (B) Amounts of radioactive compounds on TLC plates determined by a scintillation counting. Androstenedione, open circles; testosterone, closed circles.

Table 1
Activities of human P450arom

	K_m (μM)	V_{max} (nmol/(min nmol))	Reference
Androstenedione	0.26 ± 0.03	12.4 ± 0.2	This study
	0.06	5.8	[21]
	0.0014	37	[18]
	0.1[a]	14[a]	[28]
Testosterone	10.9 ± 2.4	52.2 ± 8.8	This study
	0.21	5.2	[21]

Kinetic parameters obtained in this study are compared with values previously reported.

[a] Values were obtained using a recombinant P450arom that lacked N-terminal 41 amino acids.

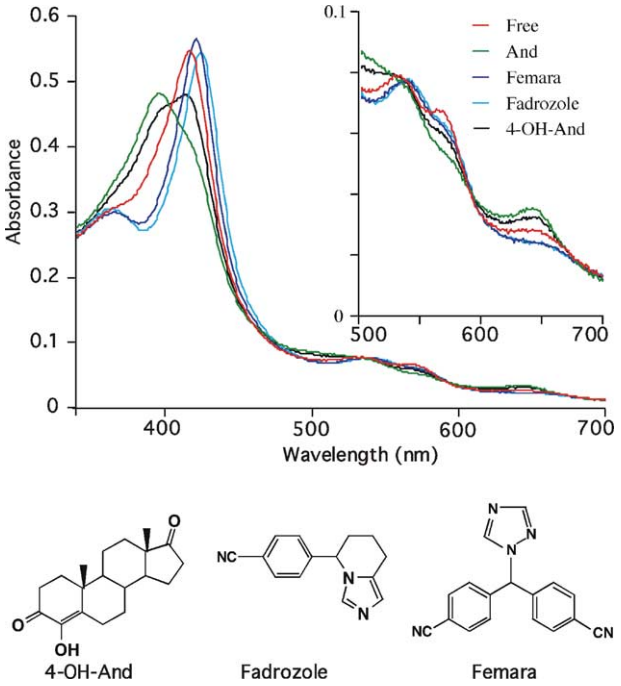

Fig. 5. Absolute spectra of purified P450arom and complexes with androstenedione and inhibitors. All spectra were recorded at room temperature with 2.7 μM P450arom in 50 mM potassium phosphate buffer (pH 7.4) containing 50 mM sodium acetate, 20% glycerol, 0.1 mM EDTA, 0.1 mM DTT, 0.3% Emulgen 913, and 1% Tween 20. Substrate-free (Free, red line), 550 μM androstenedione (And, green line), 74 μM 4-hydroxy-androstenedione (4-OH-And, black line), 55 μM Femara (blue line), 390 μM Fadrozole (cyan line), as indicated. The insert shows the expanded region of the α, β, and charge transfer bands. Chemical structures of 4-hydroxyandrostenedione, Fadrozole, Femara are shown under the chart.

showed a typical type I spectral change with a peak at 389 nm, trough at 421 nm, and a clear isosbestic point at 407 nm (Fig. 6A). Testosterone produced a similar type I spectra although the peak (386 nm) and trough (420 nm) were slightly shifted (Fig. 6B). The K_d and ΔA_{max} values obtained from double reciprocal plots of the substrate-binding spectra were 0.86±0.04 μM and 73±3 ($\Delta A_{max(389–421)}$) and 2.7±0.0.3 μM and 36±2 ($\Delta A_{max(386–420)}$) for androstenedione and testosterone, respectively (Fig. 6C).

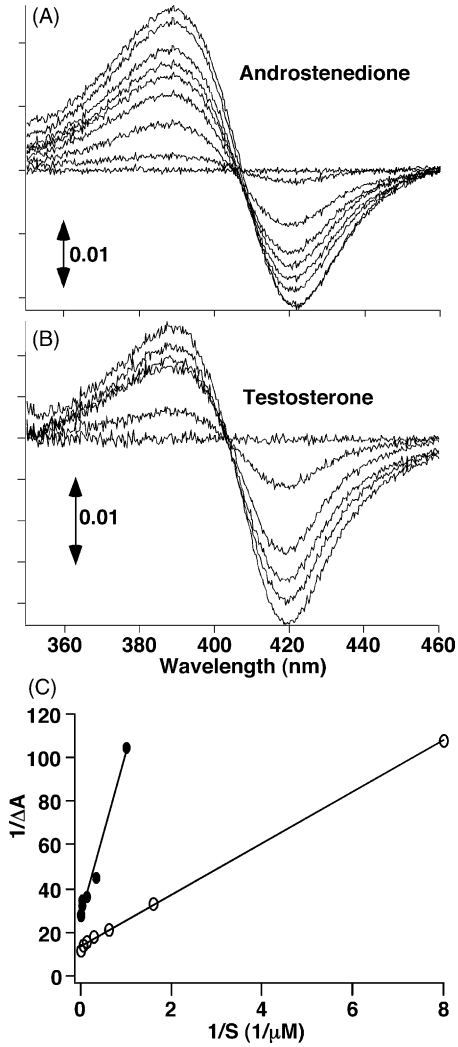

Fig. 6. Optical spectral analysis of substrate-binding complexes to human P450arom. (A) Androstenedione in 40% 2-hydroxypropyl-β-cyclodextrin solution was added to 0.56 μM P450arom to adjust the final concentrations of androstenedione to 0.14, 0.69, 1.8, 4.0, 8.5, 26, 100, 175 μM. Spectra were recorded at room temperature. (B) Testosterone in 40% 2-hydroxypropyl-β-cyclodextrin solution was added to 1 μM P450arom to adjust the final concentrations of testosterone to 1, 3, 7, 43, and 282 μM. (C) Double reciprocal plot of $\Delta A_{389–421}$ for androstenedione (open circles) and $\Delta A_{386–420}$ for testosterone (closed circles). The analysis of K_d and statistics were carried out using a software Igor Pro.

3.5. Electron paramagnetic resonance (EPR) spectra

The substrate-free form of the P450arom showed EPR signals characteristic of low-spin species at 15 K (Fig. 7). The EPR spectra indicate the presence of two species, one at $g_z = 2.48$, $g_y = 2.25$, and $g_x = 1.90$, and the other at $g_z = 2.41$, $g_y = 2.25$, and $g_x = 1.92$. Because expression was carried out from an isolated colony, purified P450arom must have a single primary sequence. Therefore, the EPR spectrum suggests that the ferric heme of human P450arom may have two low-spin conformers. Similar spectra containing multiple low-spin species have been observed for highly purified P450scc [51] and a mutant of P450cam [52]. The addition of androstenedione diminished both low-spin species and produced new signals $g_x = 8.34$, $g_y = 3.34$, $g_z = 1.63$ at 5 K, typical *g*-values of high-spin P450s [53,54]. Addition of testosterone also showed a similar high-spin spectrum ($g_x = 8.33$, $g_y = 3.37$, and $g_z = 1.63$). The slight differences in *g*-values between androstenedione- and testosterone-complexes seen in Fig. 7 may correlate to the differences observed in optical spectra (Fig. 6). The rhombicity calculated from g-values [47], 31.3 and 31.0% for androstenedione- and testosterone-P450arom complexes, respectively, is higher than those determined for P450cam (23.9%) [55], P450scc (27.0%) [51], and P450c21 (28.3%) [56].

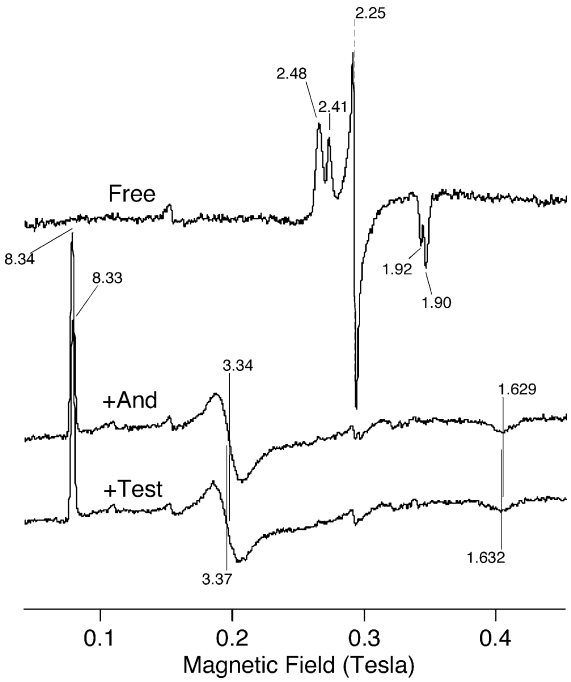

Fig. 7. EPR spectra of human P450arom NmA264R. The EPR spectra of purified P450arom (80 μM) recorded as substrate-free (Free, at 15 K), androstenedione-bound (And, at 5 K), and testosterone-bound (Test, at 5 K) forms.

4. Discussion

Overexpression of the human P450arom has been attempted by deletion of the N-terminal membrane anchor in several laboratories to obtain reasonable amounts of the purified protein [28,33,34]. However, these attempts failed because of low level of expression and/or instability of the partially purified recombinant proteins. In studies of expression of P450s in *E. coli*, a modified basic region of CYP2E1 (MARQVHSWN) has been used to replace the N-termini of CYP2C8, CYP2A6, and CYP2D6 for efficient expression [57]. Utilizing a similar N-terminal sequence from rat CYP2C11 (Fig. 1), we previously reported a successful expression of the human P450arom (NmA264C) in the presence of chloramphenicol used for the induction of cold stress response in *E. coli* [40]. Intriguingly, in the present study NmA264R could not expressed by the addition of chloramphenicol but was efficiently expressed by the coexpression of GroES/GroEL that are components of the universal folding machinery induced by heat shock in *E. coli* [58,59]. It is surprising that only a single amino acid change in the central portion of the modified human P450arom (472 amino acids) could alter so dramatically the requirement for expressing active forms of the P450 in *E. coli*. Although no association between the two forms of P450arom and breast cancer risk has been reported [60], this observation suggests that the two forms of P450arom might differently interact with molecular chaperones involved in folding machinery in human tissues, which may lead a difference in expression levels of active aromatase.

The reactions mediated by atypical P450s, allene oxide synthase [61] and thromboxane synthase [62] that do not require molecular oxygen (O_2) nor electrons from the NADPH-dependent P450 reductase, are not inhibited by CO. However, CO inhibits mono-oxygenation reactions of typical P450s that require O_2 and electrons from the reductase. The human P450arom in placental microsomal fractions is the only known exception whose reactions are not inhibited by CO [17]. The P450arom purified from human placenta also does not form the reduced CO-complex [20,21,25]. In our study, however, the reduced CO-complex of the N-terminal modified P450arom was easily detected without addition of 19-norandrostenedione [21,25] or α-naphthoflavone [63], ligands which stabilize formation of the reduced CO-complex in other studies. Without the addition of these compounds, Amarneh and Simpson [28] showed a similar CO spectrum of the human P450arom expressed in insect cells by the deletion of the N-terminal anchor. Therefore, the N-terminal anchor domain of human P450arom might interfere the formation of CO-complex in either form directly purified from placenta or heterologously expressed.

Because of stable and efficient expression, we could purify a substrate-free form of the human P450arom, which enabled us to obtain spectra of P450arom in the absence and presence of substrates and inhibitors. The majority of substrate-free P450arom was in a low-spin state although the spectrum shows a small but clear charge-transfer band (Fig. 5), suggesting that the substrate-free P450arom contains small amounts of high-spin form at room temperature. As seen in Fig. 6, androstenedione showed a typical type I spectrum, suggesting that androstenedione binds P450arom and forms a single androstenedione-P450arom complex. However, testosterone slightly shifted the peak and trough to longer wavelengths by increasing concentration. The peak and trough in the Soret region at saturation were also slightly different from those of androstenedione-complexes. A slight shift of *g*-values between androstenedione- and testosterone-complexes was also observed in EPR spectra (Fig. 7). These observations suggest a difference of heme environment between the two complexes. The higher rhombicity of substrate-bound P450arom compared with other P450s [51,55,56] is characteristic of this enzyme. If it correlates with the complex mechanism of aromatization reaction, further spectral studies using substrates and intermediates might provide information for better understanding the aromatization reaction.

Acknowledgements

This work was supported in part by NIH grants GM37942, ES00267, and by the American Cancer Society IRG-58-009-43. The authors thank Dr. F.P. Guengerich for providing a P450 reductase expression vector pOR263, and Novartis for providing aromatase inhibitors Fadrozole and Femara.

References

[1] Simpson ER, Dowsett M. Aromatase and its inhibitors: significance for breast cancer therapy. Recent Prog Horm Res 2002;57:317–38.
[2] Simpson ER, Davis SR. Minireview: aromatase and the regulation of estrogen biosynthesis: some new perspectives. Endocrinology 2001;142:4589–94.
[3] Ackerman GE, Smith ME, Mendelson CR, MacDonald PC, Simpson ER. Aromatization of androstenedione by human adipose tissue stromal cells in monolayer culture. J Clin Endocrinol Metab 1981;53:412–7.
[4] Simpson ER, Ackerman GE, Smith ME, Mendelson CR. Estrogen formation in stromal cells of adipose tissue of women: induction by glucocorticosteroids. Proc Natl Acad Sci USA 1981;78:5690–4.
[5] Tanaka S, Haji M, Nishi Y, Yanase T, Takayanagi R, Nawata H. Aromatase activity in human osteoblast-like osteosarcoma cell. Calcif Tissue Int 1993;52:107–9.
[6] Purohit A, Flanagan AM, Reed MJ. Estrogen synthesis by osteoblast cell lines. Endocrinology 1992;131:2027–9.
[7] Sasano H, Uzuki M, Sawai T, Nagura H, Matsunaga G, Kashimoto O, et al. Aromatase in human bone tissue. J Bone Miner Res 1997;12:1416–23.
[8] Bayard F, Clamens S, Meggetto F, Blaes N, Delsol G, Faye JC. Estrogen synthesis, estrogen metabolism, and functional estrogen receptors in rat arterial smooth muscle cells in culture. Endocrinology 1995;136:1523–9.
[9] Harada N, Sasano H, Murakami H, Ohkuma T, Nagura H, Takagi Y. Localized expression of aromatase in human vascular tissues. Circ Res 1999;84:1285–91.
[10] Callard GV, Petro Z, Ryan KJ. Phylogenetic distribution of aromatase and other androgen-converting enzymes in the central nervous system. Endocrinology 1978;103:2283–90.
[11] Longcope C, Billiar RB, Takaoka Y, Reddy PS, Richardson D, Little B. Tissue sites of aromatization in the female rhesus monkey. Endocrinology 1983;113:1679–82.
[12] Bulun SE, Mahendroo MS, Simpson ER. Aromatase gene expression in adipose tissue: relationship to breast cancer. J Steroid Biochem Mol Biol 1994;49:319–26.
[13] Thompson Jr EA, Siiteri PK. Utilization of oxygen and reduced nicotinamide adenine dinucleotide phosphate by human placental microsomes during aromatization of androstenedione. J Biol Chem 1974;249:5364–72.
[14] Skinner SJ, Akhtar M. The stereospecific removal of a C-19 hydrogen atom in oestrogen biosynthesis. Biochem J 1969;114:75–81.
[15] Fishman J, Guzik H, Dixon D. Sterochemistry of estrogen biosynthesis. Biochemistry 1969;8:4304–9.
[16] Townsley JD, Brodie HJ. Studies on the mechanism of estrogen biosynthesis. 3. The stereochemistry of aromatization of C19 and C18 steroids. Biochemistry 1968;7:33–40.
[17] Meigs RA, Ryan KJ. Enzymatic aromatization of steroids. I. Effects of oxygen and carbon monoxide on the intermediate steps of estrogen biosynthesis. J Biol Chem 1971;246:83–7.
[18] Hagerman DD. Human placenta estrogen synthetase (aromatase) purified by affinity chromatography. J Biol Chem 1987;262:2398–400.
[19] Hall PF, Chen S, Nakajin S, Shinoda M, Shively JE. Purification and characterization of aromatase from human placenta. Steroids 1987;50:37–50.
[20] Harada N. Novel properties of human placental aromatase as cytochrome P-450: purification and characterization of a unique form of aromatase. J Biochem 1988;103:106–13.
[21] Kellis JJ, Vickery LE. Purification and characterization of human placental aromatase cytochrome P-450. J Biol Chem 1987;262:4413–20.
[22] Nakajin S, Shinoda M, Hall PF. Purification to homogeneity of aromatase from human placenta. Biochem Biophys Res Commun 1986;134:704–10.
[23] Osawa Y, Yoshida N, Fronckowiak M, Kitawaki J. Immunoaffinity purification of aromatase cytochrome P-450 from human placental microsomes, metabolic switching from aromatization to 1 beta and 2 beta-monohydroxylation, and recognition of aromatase isozymes. Steroids 1987;50:11–28.
[24] Vickery LE, Kellis Jr JT. Aromatase cytochrome P-450. Purification and characterization of the enzyme from human placenta. Steroids 1987;50:29–36.
[25] Juchau MR, Zachariah PK. Displacement of carbon monoxide from placental cytochrome P-450 by steroids: antagonistic effects of androstenedione and 19-norandrostenedione. Biochem Biophys Res Commun 1975;65:1026–32.
[26] Corbin CJ, Graham-Lorence S, McPhaul M, Mason JI, Mendelson CR, Simpson ER. Isolation of a full-length cDNA insert encoding human aromatase system cytochrome P-450 and its expression in nonsteroidogenic cells. Proc Natl Acad Sci USA 1988;85:8948–52.
[27] Harada N. Cloning of a complete cDNA encoding human aromatase: immunochemical identification and sequence analysis. Biochem Biophys Res Commun 1988;156:725–32.
[28] Amarneh B, Simpson ER. Expression of a recombinant derivative of human aromatase P450 in insect cells utilizing the baculovirus vector system. Mol Cell Endocrinol 1995;109:R1–5.
[29] Harada N. Genetic analysis of human placental aromatase deficiency. J Steroid Biochem Mol Biol 1993;44:331–40.
[30] Lahde M, Raunio H, Pelkonen O, Karp M, Oker-Blom C. Expression of human placental cytochrome P450 aromatase (CYP19) cDNA in insect cells using a luciferase based baculovirus vector. Biochem Biophys Res Commun 1993;197:1511–7.
[31] Sigle RO, Titus MA, Harada N, Nelson SD. Baculovirus mediated high level expression of human placental aromatase (CYP19A1). Biochem Biophys Res Commun 1994;201:694–700.
[32] Jo Corbin C, Mapes SM, Lee YM, Conley AJ. Structural and functional differences among purified recombinant mammalian aromatases: glycosylation, N-terminal sequence and kinetic analysis of human, bovine and the porcine placental and gonadal isozymes. Mol Cell Endocrinol 2003;206:147–57.
[33] Osawa Y, Higashiyama T, Toma Y, Yarborough C. Diverse function of aromatase and the N-terminal sequence deleted form. J Steroid Biochem Mol Biol 1997;61:117–26.
[34] Zhang F, Zhou D, Kao YC, Ye J, Chen S. Expression and purification of a recombinant form of human aromatase from *Escherichia coli*. Biochem Pharmacol 2002;64:1317–24.
[35] Kagawa N, Kusano K, Nonaka Y. Heterologous expression of mammalian cytochrome P450 as active forms in *Escherichia coli*. Seibutsu-kogaku 2000;78:82–93.
[36] Kusano K, Waterman MR, Sakaguchi M, Omura T, Kagawa N. Protein synthesis inhibitors and ethanol selectively enhance heterologous expression of P450s and related proteins in *Escherichia coli*. Arch Biochem Biophys 1999;367:129–36.
[37] Kagawa N, Cao Q. Osmotic stress induced by carbohydrates enhances expression of foreign proteins in *Escherichia coli*. Arch Biochem Biophys 2001;393:290–6.
[38] Kagawa N, Cao Q. Stress response and foreign gene expression in *E. coli*. Recent Res Devel Biophys Biochem 2001;1:99–107.
[39] Kagawa N, Katagiri M. Expression of foreign proteins in *E. coli*: through the expression of P450s. Seikagaku 2003;75:279–84.
[40] Kagawa N, Cao Q, Kusano K. Expression of human aromatase (CYP19) in *Escherichia coli* by N-terminal replacement and induction of cold stress response. Steroids 2003;68:205–9.
[41] Nishihara K, Kanemori M, Kitagawa M, Yanagi H, Yura T. Chaperone coexpression plasmids: differential and synergistic roles of DnaK-DnaJ-GrpE and GroEL-GroES in assisting folding of an allergen of Japanese cedar pollen, Cryj2, in *Escherichia coli*. Appl Environ Microbiol 1998;64:1694–9.
[42] Imai T, Globerman H, Gertner JM, Kagawa N, Waterman MR. Expression and purification of functional human 17 alpha-

hydroxylase/17,20-lyase (P450c17) in *Escherichia coli*. Use of this system for study of a novel form of combined 17 alpha-hydroxylase/17,20-lyase deficiency. J Biol Chem 1993;268:19681–9.

[43] Shen AL, Porter TD, Wilson TE, Kasper CB. Structural analysis of the FMN binding domain of NADPH-cytochrome P-450 oxidoreductase by site-directed mutagenesis. J Biol Chem 1989;264:7584–9.

[44] Hanna IH, Reed JR, Guengerich FP, Hollenberg PF. Expression of human cytochrome P450 2B6 in *Escherichia coli*: characterization of catalytic activity and expression levels in human liver. Arch Biochem Biophys 2000;376:206–16.

[45] Tanaka M, Matsuura K, Yoshioka S, Takahashi S, Ishimori K, Hori H, et al. Activation of hydrogen peroxide in horseradish peroxidase occurs within approximately 200 micro s observed by a new freeze-quench device. Biophys J 2003;84:1998–2004.

[46] Yoshioka S, Tosha T, Takahashi S, Ishimori K, Hori H, Morishima I. Roles of the proximal hydrogen bonding network in cytochrome P450cam-catalyzed oxygenation. J Am Chem Soc 2002;124:14571–9.

[47] Tsai AL, Berka V, Chen PF, Palmer G. Characterization of endothelial nitric-oxide synthase and its reaction with ligand by electron paramagnetic resonance spectroscopy. J Biol Chem 1996;271:32563–625671.

[48] Leshin M, Baron J, George FW, Wilson JD. Increased estrogen formation and aromatase activity in fibroblasts cultured from the skin of chickens with the Henny feathering trait. J Biol Chem 1981;256:4341–4.

[49] Poulos TL, Howard AJ. Crystal structures of metyrapone- and phenylimidazole-inhibited complexes of cytochrome P-450cam. Biochemistry 1987;26:8165–74.

[50] Dawson JH, Andersson LA, Sono M. Spectroscopic investigations of ferric cytochrome P-450-CAM ligand complexes. Identification of the ligand trans to cysteinate in the native enzyme. J Biol Chem 1982;257:3606–17.

[51] Takeuchi K, Tsubaki M, Futagawa J, Masuya F, Hori H. Adrenodoxin-cytochrome P450scc interaction as revealed by EPR spectroscopy: comparison with the putidaredoxin-cytochrome P450cam system. J Biochem 2001;130:789–97.

[52] Yoshioka S, Takahashi S, Ishimori K, Morishima I. Roles of the axial push effect in cytochrome P450cam studied with the site-directed mutagenesis at the heme proximal site. J Inorg Biochem 2000;81:141–51.

[53] Tsai R, Yu CA, Gunsalus IC, Peisach J, Blumberg W, Orme-Johnson WH, et al. Spin-state changes in cytochrome P-450cam on binding of specific substrates. Proc Natl Acad Sci USA 1970;66:1157–63.

[54] Masuya F, Tsubaki M, Makino R, Hori H. EPR studies on the photoproducts of ferric cytochrome P450cam (CYP101) nitrosyl complexes: effects of camphor and its analogues on ligand-bound structures. J Biochem 1994;116:1146–52.

[55] Yoshioka S, Takahashi S, Hori H, Ishimori K, Morishima I. Proximal cysteine residue is essential for the enzymatic activities of cytochrome P450cam. Eur J Biochem 2001;268:252–9.

[56] Tsubaki M, Matsumoto N, Tomita S, Ichikawa Y, Hori H. 20beta-Hydroxy-C21-steroid 20beta-oxidase activity of cytochrome P450c21 purified from bovine adrenocortical microsomes. Biochim Biophys Acta 1998;16:197–206.

[57] Iwata H, Fujita K, Kushida H, Suzuki A, Konno Y, Nakamura K, et al. High catalytic activity of human cytochrome P450 co-expressed with human NADPH-cytochrome P450 reductase in *Escherichia coli*. Biochem Pharmacol 1998;55:1315–25.

[58] Gragerov A, Nudler E, Komissarova N, Gaitanaris GA, Gottesman ME, Nikiforov V. Cooperation of GroEL/GroES and DnaK/DnaJ heat shock proteins in preventing protein misfolding in *Escherichia coli*. Proc Natl Acad Sci USA 1992;89:10341–4.

[59] Kusukawa N, Yura T. Heat shock protein GroE of *Escherichia coli*: key protective roles against thermal stress. Genes Dev 1988;2:874–82.

[60] Miyoshi Y, Iwao K, Ikeda N, Egawa C, Noguchi S. Breast cancer risk associated with polymorphism in CYP19 in Japanese women. Int J Cancer 2000;89:325–8.

[61] Lau SM, Harder PA, O'Keefe DP. Low carbon monoxide affinity allene oxide synthase is the predominant cytochrome P450 in many plant tissues. Biochemistry 1993;32:1945–50.

[62] Wang LH, Tsai AL, Hsu PY. Substrate binding is the rate-limiting step in thromboxane synthase catalysis. J Biol Chem 2001;276:14737–43.

[63] Gartner CA, Thompson SJ, Rettie AE, Nelson SD. Human aromatase in high yield and purity by perfusion chromatography and its characterization by difference spectroscopy and mass spectrometry. Protein Expr Purif 2001;22:443–54.

[64] Kusano K, Sakaguchi M, Kagawa N, Waterman MR, Omura T. Microsomal p450s use specific proline-rich sequences for efficient folding, but not for maintenance of the folded structure. J Biochem 2001;129:259–69.

[65] Amarneh B, Corbin CJ, Peterson JA, Simpson ER, Graham-Lorence S. Functional domains of human aromatase cytochrome P450 characterized by linear alignment and site-directed mutagenesis. Mol Endocrinol 1993;7:1617–24.